Int. J. Environ. Sci. Technol. (2014) 11:1711–1722
DOI 10.1007/s13762-013-0320-2

ORIGINAL PAPER

Biosorption of ammoniacal nitrogen from aqueous solutions with low-cost biomaterials: kinetics and optimization of contact time

N. Mansuri · K. Mody · S. Basha

Received: 10 December 2012 / Revised: 20 February 2013 / Accepted: 2 May 2013 / Published online: 17 May 2013

Abstract The biosorption of ammoniacal nitrogen (N-NH_4^+) from aqueous solutions by dead biomass of brown seaweed *Cystoseira indica* and Jatropha oil cake (JOC), which is generated in the process of biodiesel recovery from its seeds, was studied under diverse experimental conditions. The N-NH_4^+ biosorption was strictly pH dependent, and maximum uptake capacity of *C. indica* (15.21 mg/g) and JOC (13.59 mg/g) was observed at initial pH 7 and 3, respectively. For each biosorbent–N-NH_4^+ system, kinetic models were applied to the experimental data to examine the mechanisms of sorption and potential rate-controlling steps. The generalized rate model and pseudo-second-order kinetic models described the biosorption kinetics accurately, and the sorption process was found to be controlled by pore and surface diffusion for these biosorbents. Results of four-stage batch biosorber design analysis revealed that the required time for the 99 % efficiency removal of 40 mg/L N-NH_4^+ from 500 L of aqueous solution were 76 and 96 min for *C. indica* and JOC, respectively. The Fourier transform infrared spectroscopy analysis before and after biosorption of ammonium onto *C. indica* and JOC revealed involvement of carboxylic and hydroxyl functional groups.

Keywords *Cystoseira indica* · Jatropha oil cake · Biosorption · Ammoniacal nitrogen kinetics · Diffusion models · Optimization

Introduction

Nitrogen is an essential nutrient for all life forms, and its presence in excess in both hydrosphere and atmosphere damages natural nutrient cycle. A recent study on European nitrogen assessment concluded that nitrogen pollution poses a greater threat to humankind than carbon pollution (Sutton et al. 2011). The main sources of nitrogen release into the environment are over-application of synthetic fertilizers (agriculture as well as aquaculture), municipal wastewater treatment, manufacture of detergents and mineral processing industries. Nitrogen compounds in aqueous environments are usually found in the form of ammoniacal nitrogen (N-NH_4^+), and it is one of the most common and toxic species of nitrogen (Rozic et al. 2000). Moreover, ammonium is classified within List II of substances under both the groundwater directive (80/68/EEC) and the dangerous substances directive (76/464/EEC) (Buss et al. 2004). Therefore, noncontrolled ammonium discharge could exert an oxygen demand in receiving waters, which can deplete dissolved oxygen, impacting the aquatic ecosystem (Zheng and Wang 2010).

The removal of N-NH_4^+ can be achieved by biological, physical and chemical methods such as biological nitrification and denitrification, filtration, adsorption, chemical precipitation, membrane, reverse osmosis, ion exchange, air stripping and breakpoint chlorination. However, these methods are impaired by low temperature in winter, complicated configuration, expensive to build and also have associated operational and maintenance problems

Electronic supplementary material The online version of this article (doi:10.1007/s13762-013-0320-2) contains supplementary material, which is available to authorized users.

N. Mansuri · K. Mody · S. Basha (✉)
Discipline of Marine Biotechnology and Ecology, CSIR-Central Salt and Marine Chemicals Research Institute, Bhavnagar 364 002, Gujarat, India
e-mail: sbasha@csmcri.org

(Boopathy et al. 2013). The adsorption removal techniques are considered as the most effective and well-established methods, including adsorption onto activated carbon, clay and zeolites (Karadag et al. 2006; Okoniewska et al. 2007; Chandra et al. 2012). Due to high cost and losses of activated carbon in the application processes and the low abundance of zeolite and clay in many countries, there is growing interest in using cheaper, abundantly available, easily regenerable and biodegradable alternative materials.

Cystoseira indica, an abundantly available seaweed along Saurashtra–Kachchh coast of India, and Jatropha oil cake (JOC), which is a by-product during recovery of biodiesel from seeds of Jatropha plant, have been used as effective biosorbents for the removal of heavy metals, organics and dyes (Namasivayam et al. 2007; Basha et al. 2009). Hence, there is a strong need for further studies using these low-cost biomaterials to remove $N\text{-}NH_4^+$ from wastewaters. Besides their cost and availability, they could be promoted as compost and fertilizer after ammonium biosorption.

The main focus of this study is to evaluate the effects of pH, reaction time and biosorbent dosage on $N\text{-}NH_4^+$ removal using both *C. indica* and Jatropha oil cake. In addition, external mass transfer diffusion and intraparticle mass transfer diffusion models were used to identify the main rate-controlling steps in the overall uptake mechanism. A design analysis method is proposed to optimize the contact time for the design of a biosorption system for removal of $N\text{-}NH_4^+$.

This research has been performed during December 2011 to April 2012 in the laboratory of Marine Biotechnology and Ecology discipline of CSIR-Central Salt and Marine Chemicals Research Institute, Bhavnagar, Gujarat, India.

Materials and methods

Materials

The chemicals used in this study were of analytic reagent grade. The stock solution of 1,000 mg/L $N\text{-}NH_4^+$ was prepared by dissolving 3.819 g ammonium chloride salt (NH_4Cl) in Millipore water. The working solutions of different concentrations were prepared by diluting the stock solution with Millipore water. In order to obtain the NH_4–N solution of different initial pH values, small amounts of 0.1 N HCl or NaOH (S.D. Fine Chem, India) were added.

Preparation of biosorbents

The brown alga *C. indica* was collected from the Saurashtra coast of Gujarat (Veraval), India, in December 2005. The alga was washed twice with running water and five times with deionized water. The washed biomass was oven-dried at 60 °C for 24 h, crushed with an analytical mill, sieved (size fraction of 0.50–0.60 mm) and stored in polypropylene bottles until use.

Jatropha curcas L press cake, obtained from biodiesel plant within the institute, was washed several times with tap water to remove physical impurities and then dried in oven overnight at 120 °C. The dry biomass was soaked in KOH solution for 24 h and subjected to a two-step heating process at 120 °C for 2 h in an oven and then at 500 °C for 4 h in a furnace. The resultant biosorbent was crushed, sieved (size fraction of 0.85–0.95 mm), stored in glass bottle and used in experiments.

Batch biosorption experiments

All the experiments were conducted at a constant temperature of 25 ± 1 °C to furnish environmentally relevant conditions. The effect of solution pH on the equilibrium uptake of ammonium from aqueous solution by biosorbents was investigated between pH 2 and 10, by adjusting with HCl and NaOH solutions. The experiments were performed by adding a known weight of biosorbent into 250-mL Erlenmeyer flasks containing 20 mg/L of NH_4–N. The flasks were shaken at 190 rpm and 298 K for 24 h to attain equilibrium, and the amount of ammonium remaining in solution was measured by the conventional Nesslerization method using a UV–Vis spectrophotometer (Shimadzu, UV-1201) at 610 nm after the separation of biosorbent by membrane filtration (Millipore 0.45 mm pore size) (APHA 1998).

The kinetics of sorption studies were conducted with 250 mL of ammonium solution with initial concentrations of 10, 20 and 40 mg/L. The samples were withdrawn at regular intervals, and the residual concentration of ammonium in the aqueous phase was analyzed after membrane filtration.

Equilibrium sorption experiments were performed in 250-mL flasks containing ammonium solution (100 mL) of known concentrations (10–80 mg/L). Weighed amounts of biosorbent (500 mg) were added to each flask, and the mixtures were agitated on the rotary shaker. After 24 h of agitation, the solution was separated from the biosorbent by membrane filtration and analyzed for $N\text{-}NH_4^+$.

The effect of $N\text{-}NH_4^+$ sorption by the membrane filter during the filtration process was minimized by discarding the first 25 mL portion of the ammonium solution. The subsequent portion was used for the measurement of absorbance for ascertaining $N\text{-}NH_4^+$ concentration. All the biosorption experiments were repeated twice to substantiate the results with controls. Controls were employed to ensure that sorption was by biosorbent only, and to evaluate the eventual ammonium losses through volatilization

to ammonia due to stirring or pH. The blank experiments demonstrated that the biosorbent did not contain free nitrogen and the NH_4–N mass losses due to the stirring were less than 3 % for the studied concentration range (10–80 mg/L). Moreover, pH variation between 3 and 11 did not cause significant N-NH_4^+ volatilization to ammonia (<3 %).

FT-IR and SEM studies

Infrared spectra of N-NH_4^+-biosorbed and raw biomasses of both *C. indica* and JOC were obtained using a Fourier transform infrared spectrometer (FT-IR GX 2000, Perkin-Elmer). Before the analysis, the wet samples were freeze-dried, and 30 mg of finely ground biomass was pelleted with 300 mg of KBr (Sigma) in order to prepare translucent sample disks. The FT-IR spectra were recorded over the wave number range 400–4,000/cm with 10 scans at a resolution of 4/cm.

The surface structure of biosorbents before and after ammonium sorption was analyzed by scanning electron microscopy (SEM) coupled with energy-dispersive X-ray analysis (EDX) using a JEOL 5600 LV SEM. Samples were mounted on a stainless steel stab with a double-stick tape followed by sputter coating gold to improve conductivity to increase the electron conduction and to improve the quality of the micrographs.

Biosorption capacity

The amount of NH_4–N^+ sorbed at equilibrium, q_e (mg/g) which represents the uptake, was calculated from the difference in N-NH_4^+ concentration in the aqueous phase before and after biosorption, as per the following equation:

$$q_e = \frac{V(C_i - C_e)}{W} \quad (1)$$

where V is the volume of N-NH_4^+ solution (L), C_i and C_e are the initial and equilibrium concentrations of ammonium in solution (mg/L), respectively, and W is the mass of dry biosorbent (g).

Nonlinear regression analysis

All the model parameters were evaluated by nonlinear regression using DATAFIT® software (Oakdale Engineering, USA). The optimization procedure required an error function to be defined in order to be able to evaluate the suitability of the equation to the experimental data. Apart from the regression coefficient (R^2), the residual or sum of square error (SSE) and the standard error (SE) of the estimate were also used to gauge the goodness of fit. SSE can be defined as:

$$\mathrm{SSE} = \sum_{i=1}^{m} (Q_i - q_i)^2 \quad (2)$$

SE can be defined as:

$$\mathrm{SE} = \sqrt{\frac{1}{m-p}\sum_{i=1}^{m} (Q_i - q_i)^2} \quad (3)$$

where q_i is the observation from the batch experiment i, Q_i is the predicted value from the isotherm for corresponding q_i, m is the number of observations in the experimental isotherm, and p is the number of parameters in the regression model. The smaller SE and SSE values indicate the better curve fitting.

Results and discussion

Sorption potential of *C. indica* and JOC

The results exhibited that both the biosorbents, *C. indica* and JOC, were able to remove the N-NH_4^+ from aqueous solutions with high efficiency (15.21 and 13.59 mg/g for *C. indica* and JOC, respectively). The removal of various adsorbents has been studied extensively, and ammonium sorption capacities were reported (Table 1). Although the published values were obtained under different experimental conditions, they may be useful as a template for comparing the adsorption capacities. The experimental biosorption capacity of *C. indica* obtained in this study is higher than that of most of the adsorbents including activated carbon except hydrogels (Zheng and Wang 2010; Zheng et al. 2011). The high biosorption capacity of *C. indica* conveys that it has great potential for application in ammonium removal from wastewater.

Effect of pH

The removal of NH_4^+ ions from aqueous solutions by both *C. indica* and JOC was studied under different pH conditions in the range of 3–11 (Fig. 1). The optimum range of pH varied from 3 to 7 with the biosorption capacities ranged from 7.05 to 9.21 mg/g and 8.70–5.54 mg/g for *C. indica* and JOC, respectively. For the pH above 7, ammonium biosorption capacity was declined rapidly for both *C. indica* and JOC; however, highest biosorption capacity of JOC was achieved at pH 3. This can be attributed to the difference between the chemical properties and functional groups present on the surface of *C. indica* and JOC. In fact, at pH < 5, the surface may get positively charged, thus making (H^+) ions compete effectively with ammonium cations causing a decrease in the biosorption capacity (Wu et al. 2006). At higher pH (5–7) the

Table 1 Results of some ammonium adsorption on various sorbents

Adsorbent	Sorption capacity (mg/g)	pH	Reference
P. oceanica fibers	1.73	6	Jellali et al. (2011)
P. tricuspidata	6.59	5–8	Liu et al. (2010)
Sawdust	1.7	6.0	Wahab et al. (2010)
Natural zeolite	8.91	–	Lebedynets et al. (2004)
Natural Australian zeolite	2.0	5.5	Komarowski and Yu (1997)
Clinoptilolite	14.5	7.5	Tosun (2012)
Natural Turkish clinoptilolite	2.5	7.0–7.5	Demir et al. (2002)
Natural Turkish clinoptilolite	2.9	–	Karadag et al. (2006)
Coconut shell-activated carbon	2.06–2.3	9.0	Boopathy et al. (2013)
Local activated carbon	0.08	7.0	Okoniewska et al. (2007)
Silty loam soil	0.91	8.0	Fernando et al. (2005)
Sandy loam soil	0.22	8.2	Fernando et al. (2005)
Hydrogel (polyvinyl alcohol, acrylic acid and tourmaline)	33.81	4–8	Zheng et al. (2011)
Biotite-based hydrogel composite	32.87	4–9	Zheng and Wang (2010)
C. indica	15.21	5.0	Present study
Jatropha oil cake	13.59	3.0	Present study

biosorbent surface may get negatively charged, enhancing the biosorption of positively charged ammonium through electrostatic forces of attraction. Previous studies reported that the ranges of optimum pH for ammonium adsorption by zeolite, clinoptilolite and activated carbon were 6–7, 5–7 and 7–9, respectively (Rozic et al. 2000; Ji et al. 2007). Ammonium biosorption was decreased above pH 7 due to the reaction of NH_4^+ ions with OH^- ions according to Eqs. (4) and (5):

$$NH_4^+ + OH^- \leftrightarrow NH_3 + H_2O \quad (4)$$

$$NH_3 + H_3O^+ \rightarrow NH_4^+ + OH^- \quad (5)$$

Also, for pH above 7, the NH_4^+ concentration diminishes, equilibrium shifts toward the formation of ammonia gas, and these conditions become increasingly less congenial (Emmerson et al. 1981; Thornton et al. 2007). As the initial pH of NH_4^+ solution is near 7.0, the pH of solution was not adjusted in the subsequent experiments.

Effect of biosorbent dosage

The dependence of N-NH_4^+ sorption on biosorbent dose is studied by varying the amount of adsorbent from 0.25 to 1.5 g while keeping all other variables (pH, agitation time and concentration) constant (Fig. 2). As the biosorbent dose was increased from 0.25 to 1.5 g/L for *C. indica* and JOC, the equilibrium biosorption amount decreased from 12.56 to 3.41 mg/g and 11.20–2.74 mg/g, respectively. The decrease in biosorption capacity with increasing dose could be ascribed to two reasons (Tuzun et al. 2005). First, with

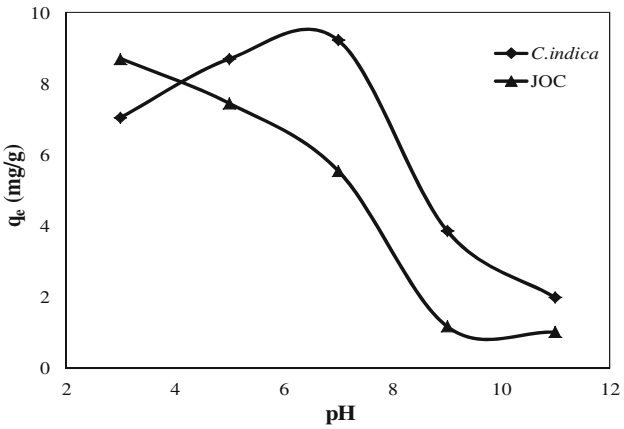

Fig. 1 Effect of pH on N-NH_4^+ biosorption onto *C. indica* and JOC

increasing biosorbent dose there were a decrease in total surface area of the biosorbent and an increase in diffusion path length due to aggregation of biosorbent particles. The aggregation becomes increasingly significant as the weight of the biosorbent is increased. Secondly, the increase in biosorbent dose at constant ammonium concentration and volume will lead to unsaturation of biosorption sites through the sorption process. Similar conclusions have been drawn by Donmez and Aksu (2002) in biosorption with algae; that is, an increase in biosorbent dose reduces the amount of metal recovered per dry weight unit of biosorbent used. These results suggest that the equilibrium sorption capacity of each biosorbent is a function of its weight.

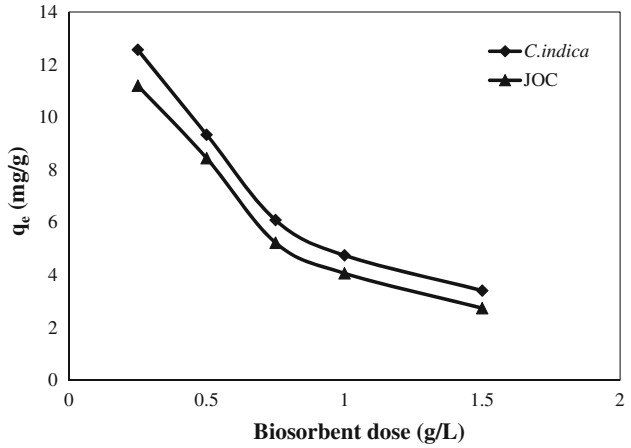

Fig. 2 Effect of biosorbent dose on N-NH_4^+ biosorption onto *C. indica* and JOC

Effect of contact time on biosorption

The biosorption rate was rapid for the initial contact period of 30 min for *C. indica* and 50 min for JOC (more than 90 % of the maximum biosorbed amount was attained for all experiments), and thereafter, the N-NH_4^+ uptake process tends to proceed at a slower rate before finally reaching equilibrium (Fig. 3a, b for *C. indica* and JOC, respectively). The fast biosorption at the initial stage may be due to the fact that a large number of vacant surface sites are available for sorption and then the remaining surface sites are difficult to be occupied because of the repulsion between the N-NH_4^+ on the *C. indica*/JOC and bulk phase. Moreover, the slowdown can be attributed to decelerating biosorption driving force, that is, the lower concentration gradient of the adsorbate (Aliabadi et al. 2012). The equilibrium biosorption of N-NH_4^+ on *C. indica* and JOC was achieved within 50 and 90 min, respectively. Taking into account the effect of divergent factors, the equilibration period of 3 h was selected for all further experiments. The optimum equilibrium time determined in the present study was consistent with the published reports on the adsorption of N-NH_4^+ on various zeolites as well as marine magnoliophyta biomass (Wu et al. 2006; Ji et al. 2007; Wahab et al. 2010). The influence of the initial NH_4-N concentration on biosorption dynamics showed that the biosorption capacity of both *C. indica* and JOC increased from 3.84 to 12.64 mg/g and 3.06 to 11.69 mg/g, respectively, as the initial N-NH_4^+ concentration increased from 10 to 40 mg/L. The increase in adsorbate concentration results in greater driving force which increases the biosorption capacity (Lim et al. 2010).

Kinetic modeling based on chemical reaction

In order to identify the mechanism involved during the present biosorption process and the potential rate-

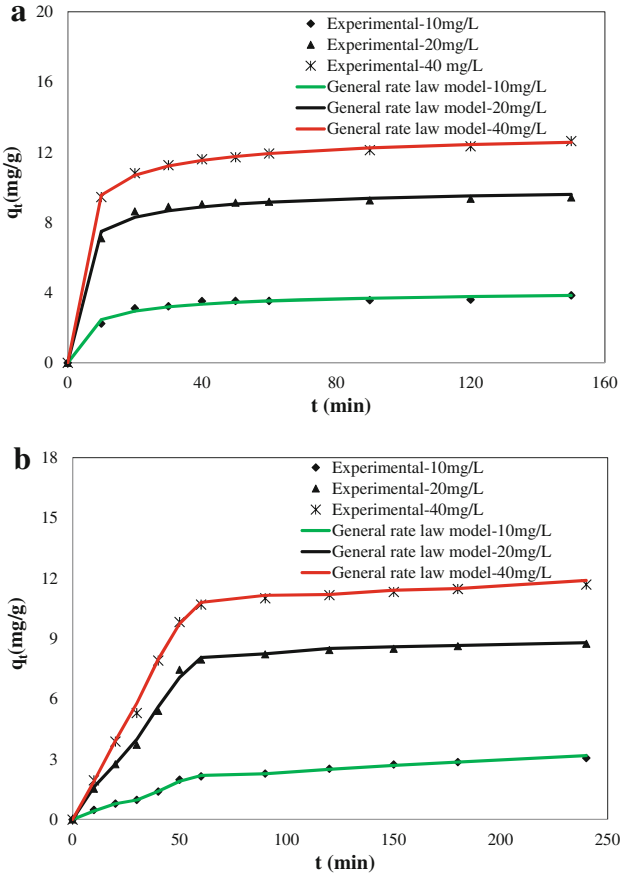

Fig. 3 **a** Biosorption kinetics for sorption of N-NH_4^+ onto *C. indica* at three different concentrates. **b** Biosorption kinetics for sorption of N-NH_4^+ onto JOC at three different concentrations

controlling steps such as mass transport, pore diffusion and chemical reaction processes, various kinetic models were used to dovetail the experimental data (provided as supplementary data). The best-apt model was selected based on nonlinear regression correlation coefficient (R^2), SE and SSE values as well as the calculated q_e values.

The most widely used kinetic models based on reaction order are pseudo-first-order model proposed by Lagergren (1898) and Ho and McKay's pseudo-second-order model (Ho and McKay 1999). The first-order rate expression of Lagergren is used when the rate of occupation of binding sites is proportional to the number of unoccupied sites on the biosorbent and is generally applicable over the first 20–30 min of the sorption process. The pseudo-second-order equation is based on the sorption capacity of the solid phase and predicts the "chemisorption" behavior over the entire time adsorption (Ho and McKay 1999). Liu and Liu (2008) proposed the general rate law model which states that the kinetic order of a biosorption reaction of known and unknown mechanism must be experimentally determined without the necessity of a prior assumption of the

Table 2 Parameters of kinetic models for ammonium biosorption on *C. indica* and JOC

Models	*C. indica*			JOC		
	$C_i = 10$ mg/L	$C_i = 20$ mg/L	$C_i = 40$ mg/L	$C_i = 10$ mg/L	$C_i = 20$ mg/L	$C_i = 40$ mg/L
q_e (experimental, mg/g)	3.84	9.41	12.64	3.06	8.74	11.69
Pseudo-first-order						
k_1 (min^{-1})	0.019	0.034	0.025	0.023	0.025	0.029
q_e	1.416	2.574	4.248	1.322	2.367	3.914
R^2	0.653	0.816	0.801	0.926	0.932	0.905
SE	0.591	0.677	0.523	0.418	0.416	0.479
SSE	2.443	3.208	1.9118	1.574	1.559	2.069
	5.841	36.71	173.26	7.152	29.364	146.1
Pseudo-second-order						
q_e (mg/g)	4.374	10.36	13.66	2.446	13.46	15.45
k_2 (g/mg/min)	0.0002	0.004	0.056	0.001	0.018	0.032
R^2	0.987	0.893	0.899	0.984	0.891	0.988
SE	0.228	0.329	0.287	0.214	0.393	0.236
SSE	0.364	0.622	0.416	0.319	0.715	0.349
Generalized rate model						
q_e (mg/g)	4.074	9.674	12.96	3.44	9.06	11.93
k_n (g/mg/min)	0.458	0.502	0.559	0.018	0.020	0.023
n	2.241	2.301	2.146	2.014	2.120	2.317
R^2	0.991	0.992	0.996	0.995	0.991	0.998
SE	0.071	0.076	0.089	0.084	0.070	0.095
SSE	0.002	0.002	0.003	0.003	0.002	0.004
Intraparticle diffusion						
k_{ip1} ($mg/g/min^{0.5}$)	0.618	1.705	2.150	0.352	1.502	2.002
I (mg/g)	0.114	0.561	0.834	−0.763	−3.859	−4.768
R^2	0.973	0.946	0.929	0.951	0.984	0.988
SE	0.295	1.188	1.523	0.152	0.356	0.4137
SSE	0.174	2.827	3.942	0.093	0.502	0.685
k_{ip2} ($mg/g/min^{0.5}$)	0.045	0.061	0.166	0.085	0.116	0.128
I (mg/g)	3.190	8.678	10.565	1.114	7.442	9.905
R^2	0.913	0.986	0.985	0.979	0.969	0.998
SE	0.074	0.018	0.053	0.049	0.041	0.011
SSE	0.022	0.002	0.012	0.007	0.005	0.004
External mass transfer						
k_f (cm/s)	0.23×10^{-3}	0.46×10^{-3}	0.82×10^{-3}	0.17×10^{-3}	0.29×10^{-3}	0.47×10^{-3}
R^2	0.863	0.873	0.843	0.901	0.899	0.802
SE	0.835	0.757	0.980	0.613	0.770	0.992
SSE	1.647	1.347	1.957	1.102	1.474	2.112
Pore and surface diffusion						
D (cm^2/s)	1.16×10^{-8}	2.02×10^{-8}	3.39×10^{-8}	0.94×10^{-8}	1.38×10^{-8}	2.25×10^{-8}
R^2	0.797	0.822	0.815	0.789	0.827	0.817
SE	1.341	1.121	1.181	1.362	1.112	1.189
SSE	4.122	3.272	3.622	4.121	3.271	3.622
Biot number (B_N)	109.05	125.25	133.03	162.77	189.14	188

order of reaction, as in two previous models. This model presents the reaction order in integers or in noninteger, rational numbers.

The calculated kinetic constants along with statistical parameters for various kinetic models are presented in Table 2. For the pseudo-first-order model, the regression

coefficients (R^2) were relatively low and varied from 0.653 to 0.816. Furthermore, the experimental biosorbed capacities were two to three times higher than the theoretical values. Consequently, biosorption of ammonium onto *C. indica* and JOC is not an ideal pseudo-first-order reaction. Similar results were obtained for ammonium sorption onto natural Turkish clinoptilolite (Karadag et al. 2006) and *Posidonia oceanica* L. fibers (Jellali et al. 2011). Kinetic parameters of the pseudo-second-order equation were characterized by higher regression coefficients (0.891–0.988) and lower values of SE (0.214–0.393) and SSE (0.319–0.715), which support improved adjustment of that model to experimental data of both *C. indica* and JOC. Increase in sorption capacity of *C. indica* and JOC with increasing initial concentration of N-NH_4^+ (from 3.938 to 23.41 mg/g) was observed. This may be attributed to increase in biosorption process driving force (Nethaji et al. 2012).

In comparison, the generalized rate model regression coefficient (R^2) values were significantly higher and ranged from 0.991 to 0.998, while SE and SSE values were lower and ranged from 0.070 to 0.095 and 0.002 to 0.004, respectively. The high R^2 and low SE and SSE values as well as the good agreement between the experimental and predicted equilibrium sorption capacities confirm better suitability to the generalized rate model (Fig. 3a, b for *C. indica* and JOC, respectively). Liu and Wang (2008) opined that the reaction order must be set on the basis of the experimental results and it is inappropriate to first set the order of reaction and then to adjust a model. Values of reaction order varied from 2.14 to 2.24 and 2.01 to 2.24 for *C. indica* and JOC, respectively, depending on the initial concentration of N-NH_4^+. Similar results were obtained by Kumar and Gaur (2011), and they concluded that generalized rate model failed to accurately illustrate the kinetics of metal biosorption due to unjustifiable change in rate constant and reaction order with varying concentrations of metal and biomass in the solution. However, the change in both reaction order and kinetic constant in the present work is marginal and expected as the parameter that precludes the process may be a number of active places on the surface of biosorbents (Witek-Krowiak 2011).

Kinetic modeling based on diffusion

Sorption of any sorbate molecule on sorbent particles essentially involves diffusive transport of the component mass from the bulk through the boundary layer close to the surface of the sorbent, intraparticle diffusion and binding of the molecules to the active sites in sorbent pores. The quickest stage is bonding to the active sites, and it is assumed that this stage does not limit mass transfer. Thus, only external mass transfer and intraparticle diffusion play important role in rate determination. It is necessary to evaluate the diffusion coefficients using diffusion-based models for design of efficient biosorption system (Sun et al. 2012).

Intraparticle diffusion model

A widely accepted intraparticle diffusion (IPD) model developed by Weber and Morris (1963) was applied to the experimental data, and the parameters obtained are presented in Table 1. The IPD model was characterized using the relationship between specific sorption (q_t) and the square root of time ($t_{1/2}$) by Eq. (6):

$$q_t = k_{ip} t^{0.5} + I \tag{6}$$

where k_{ip} is the intraparticle rate constant (mg/g/$min^{0.5}$) and I is the intercept. The intraparticle diffusion model implies that the plot of q_t versus $t^{0.5}$ should be linear and the particle diffusion would be the controlling step if this line passed through the origin (Gupta et al. 2009).

Both *C. indica* and JOC showed similar behavior, and each curve presented two linear portions (Fig. 4a, b for

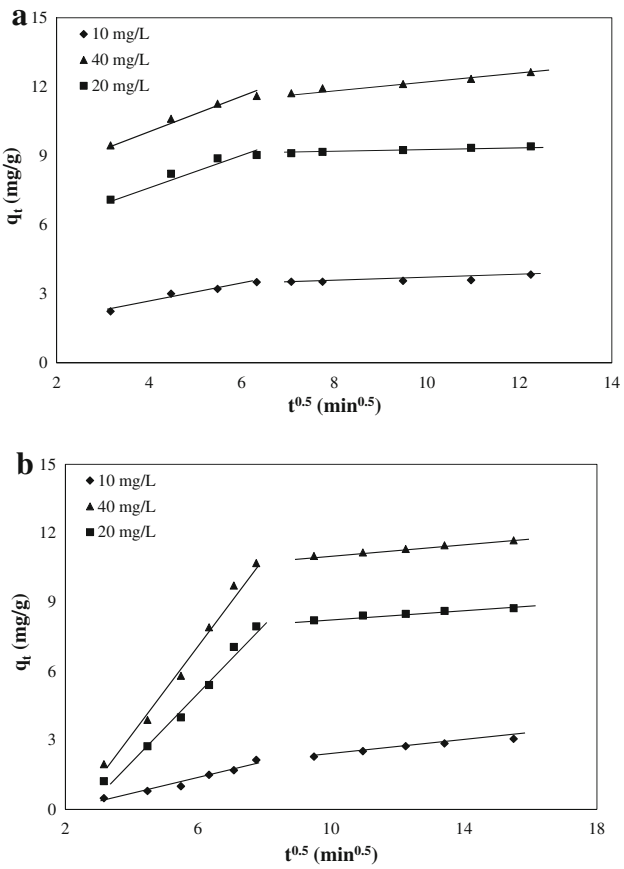

Fig. 4 **a** Intraparticle diffusion plots for the biosorption of N-NH_4^+ onto *C. indica* at three different concentrations. **b** Intraparticle diffusion plots for the biosorption of N-NH_4^+ onto JOC at three different concentrations

C. indica and JOC, respectively). At the beginning of the N-NH_4^+ diffusion into biosorbents, there was a fast initial uptake with moderate intraparticle diffusion rate constants (0.62–2.15 mg/g/$min^{0.5}$ and 0.35–2.0 mg/g/$min^{0.5}$ for *C. indica* and JOC, respectively). It accounted for more than 70 % of the overall biosorption, regardless of the variation in system operating conditions. This could be explained by the large concentration gradient and availability of surface sites on biosorbents in the initial stage of the whole biosorption process. When the biosorption process continued, available surface sites in micropore region of biosorbents were reduced, due to biosorbed N-NH_4^+ molecules on biosorbent surface blocking certain micropores. The second portion has lower intraparticle diffusion constants (0.045–0.166 mg/g/$min^{0.5}$ and 0.085–0.128 mg/g/$min^{0.5}$ for *C. indica* and JOC, respectively), which implied that the micropores of biosorbents were almost fully occupied by N-NH_4^+ molecules. These adsorbates will start attaching to the active site on the mesopores and hence give rise to a flat and long linear portion. A high R^2 (0.913–0.998), low SE (0.011–1.523) and SSE (0.004–3.942) values suggest a significant relationship between q and $t^{0.5}$ for N-NH_4^+ at all the three tested concentrations for both *C. indica* and JOC. Intraparticle diffusion rate constants varied with change in concentration of N-NH_4^+, and this phenomenon could be attributed to change in diffusion driving force (Wu et al. 2006). The value of intercept *I* also increased with increasing concentration of N-NH_4^+ in the solution for both *C. indica* and JOC. This happened because a high N-NH_4^+ concentration seems to have provided better driving force to external mass transfer process (Benaissa and Elouchdi 2011). The intraparticle diffusion model curves do not pass through the origin, which is an indication that N-NH_4^+ diffusion in the bulk of the biosorbent is not the only process that governs the biosorption and external mass transfer has also played a pivotal role in N-NH_4^+ sorption by both *C. indica* and JOC (Vijayaraghavan et al. 2008).

External mass transfer model

The diffusion of a compound at the surface and in the pores of sorbents plays a key role during biosorption. Two kinetic models have been used to evaluate the contribution of this phenomenon:

1. external diffusion model characterized by Eq. (7) (Dizge et al. 2008):

$$\frac{C_t}{C_e} = e^{-k_f(S/V)t} \tag{7}$$

2. pore and surface mass diffusions are well described by Fick's second law of diffusion from which Eq. (8) is derived (Urano and Tachikawa 1991; Ponnusami et al. 2010):

$$-\log\left(1-\left(\frac{q_t}{q_e}\right)^2\right) = \left(\frac{4\pi^2 D}{2.3\phi^2}\right) \tag{8}$$

where C_i and C_t, respectively, represent the initial concentration and at time t (mg/L), k_f (cm/s) is the external mass transfer coefficient, D (cm^2/s) is the sum of pore and surface diffusion, and S/V (cm^{-1}) represents the ratio of the total interfacial area of the particles against the total solution volume; this ratio can be determined by Eq. (9) below:

$$\frac{S}{V} = \frac{3L}{\rho\phi} \tag{9}$$

where L is the biosorbent concentration (kg/m^3), ϕ the mean particle diameter (cm), and ρ the apparent density of the biosorbent (kg/m^3). Since the particles of *C. indica* and JOC, used in this study, have a diameter ranging from 0.50 to 0.60 mm and 0.85 to 0.95 mm, respectively, the values used for the kinetic modeling were the mean of these extreme values (0.55 and 0.90 mm).

In order to check whether the internal diffusion mechanism is the main process that governs the biosorption of NH_4–N, the Biot number (B_N) was calculated according to Eq. (10):

$$B_N = k_f \frac{\phi}{D} \tag{10}$$

When B_N is greater than 100, the process can be assumed to proceed mainly by internal diffusion mechanism (Dizge et al. 2008). The values of k_f (2.962×10^{-3}–4.744×10^{-3} cm/s), D (1.769×10^{-8}–3.215×10^{-8} cm^2/s) and B_N calculated from the above Eqs. (7)–(10) are given in Table 1. If the value of D lies in the range 10^{-13}–$10^{-5}cm^2$/s as it is the case here, it indicates that chemisorption phenomena occur during the biosorption process (Dizge et al. 2008). This result substantiates the previous result on satisfactory fit of the pseudo-second-order model, which is governed by chemisorption, to the kinetic data. N-NH_4^+ biosorption is best described by the internal diffusion mechanism rather than the external diffusion since the value of B_N for both *C. indica* and JOC (109–189) was greater than 100 (Langmuir 1918). The high regression coefficients (0.895–0.924) obtained with pore and surface mass diffusion model are in agreement with this conclusion.

Multistage batch adsorption design

Kinetic equations can be used to predict the design of multistage crosscurrent batch biosorption systems (Ho and McKay 1998; Li et al. 2010). The time required for the biosorption process for each stage is critical in both the design of the biosorption equipment and its application on a large scale. A typical example was considered for the

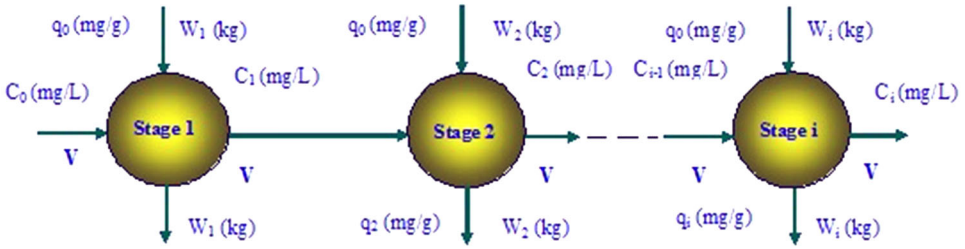

Fig. 5 Schematic diagram of a multistage batch biosorption system

removal of 99 % N-NH_4^+ from 500 L of 40 mg/L of the wastewater in four stages of a batch biosorption process.

The wastewater to be treated contains V volume (L) of solution, and an initial N-NH_4^+ concentration C_0 (mg/L) entered the first batch biosorber using an amount W_1 (kg) with q_0 (mg/g) loading of initial N-NH_4^+. After reaching biosorption equilibrium and then separation, the V(L) solution with N-NH_4^+ concentration C_1 (mg/L) entered the second biosorber with W_2 (g) of adsorbent and q_0 (mg/g) N-NH_4^+ loading to be biosorbed and separated again, and so on (Fig. 5). The solution concentration of the wastewater from each biosorber became C_i (mg/L). The N-NH_4^+ loading on the biosorbent for each stage increased from q_0 to q_i (mg/g). When fresh biosorbent was used, $q_0 = 0$ and the mass balance at each stage in a multistage adsorption system can be expressed as:

$$V(C_{i-1} - C_i) = W(q_{t,i} - q_0) \tag{11}$$

where n is the sequence number of biosorption stage ($i = 1, 2,3, \ldots, N$). When the biosorption comes to equilibrium, C_i is the N-NH_4^+ solution equilibrium concentration at the ith stage, and W_i and q_i are the biosorbent amount and the N-NH_4^+ equilibrium loading on the biosorbent, respectively, at the nth stage, namely $C_i = C_{ei}$ and $q_i = q_{ei}$.

When fresh sorbents are used at each stage and the pseudo-second-order equation is used to describe equilibrium in the multistage sorption system, then the mass balance equation can be obtained by combining the pseudo-second-order rate equation and (11):

$$C_i = C_{i-1} - \frac{Wkq_{e,i}^2 t}{V(1 + kq_{e,i}^2 t)} \tag{12}$$

The total amount of NH_4–N removal can be calculated analytically as follows:

$$\sum_{i=1}^{N} C_{i-1} - C_i = \sum_{i-1}^{N} \frac{Wkq_{e,i}^2 t}{V(1 + kq_{e,i}^2 t)} \tag{13}$$

The N-NH_4^+ removal, R_i, in each stage can be evaluated from the equation as follows:

$$R_i = \frac{100(C_{i-1} - C_i)}{C_0} = \frac{100Wkq_{e,i}^2 t}{VC_0(1 + kq_{e,i}^2 t)} \tag{14}$$

The total removal of NH_4–N can be calculated analytically as follows:

$$\sum_{i-1}^{N} R_i = \frac{100W}{VC_0} \sum_{i=1}^{N} \frac{kq_{e,i}^2 t}{(1 + kq_{e,i}^2 t)} \tag{15}$$

It is useful for process design purposes if q_e and k can be expressed as a function of C_0, as follows:

$$q_e = X_{qe} C_o^{Yq} \tag{16}$$

$$k = X_k C_o^{Yk} \tag{17}$$

Substituting the values of q_e and k from Eqs. (16) and (17) into Eqs. (14) and (15) gives

$$R_i = \frac{100S(X_k C_{i-1}^{yk})(X_q C_{i-1}^{yk})^2 t}{VC_0(1 + X_q C_{i-1}^{yq})t} \tag{18}$$

$$\sum_{i=1}^{N} R_i = \frac{100S}{VC_0} \sum_{i=1}^{N} \frac{(X_k C_{i-1}^{yk})(X_q C_{i-1}^{yq})^2 t_i}{VC_0(1 + X_q C_{i-1}^{yq})t_i} \tag{19}$$

Eqs. (15) and (19) can be used to predict the removal of N-NH_4^+ at any given initial concentration and the reaction time for any multistage system.

When data of q_e and k against initial N-NH_4^+ concentration, C_0, were regressed, the following equations were obtained for *C. indica* and JOC:

$$C.\,indica: \begin{array}{ll} q = 0.6463C_0^{1.16} & R^2 = 0.925,\ \mathrm{SE} = 0.809 \\ k = 5.227C_0^{-0.239} & R^2 = 0.999,\ \mathrm{SE} = 0.596 \end{array} \tag{20}$$

$$\mathrm{JOC}: \begin{array}{ll} q = 0.797C_0^{1.55} & R^2 = 0.999,\ \mathrm{SE} = 0.672 \\ k = 4.667C_0^{-0.312} & R^2 = 0.942,\ \mathrm{SE} = 0.818 \end{array} \tag{21}$$

When Eqs. (20) and (21) were incorporated into Eq. (19), the model equations become

$$\sum_{i=1}^{N} R_n = \frac{100S}{VC_0} \sum_{i=1}^{N} \frac{(5.227C_{i-1}^{-0.239})(0.646C_{i-1}^{1.159})^2 t_i}{\left[1 + (5.227C_{i-1}^{-0.312})(0.646C_{i-1}^{1.159})^2 t_i\right]} \tag{22}$$

$$\sum_{i=1}^{N} R_n = \frac{100S}{VC_0} \sum_{i=1}^{N} \frac{(4.667C_{i-1}^{-0.312})(0.797C_{i-1}^{1.155})^2 t_i}{\left[1 + (4.667C_{i-1}^{-0.312})(0.797C_{i-1}^{1.155})^2 t_i\right]} \tag{23}$$

Equation (23) is a mathematical model for the calculation of contact time for the second, third and fourth stages of a four-stage batch biosorption of N-NH_4^+ onto *C. indica*/JOC. A series of contact times from 2 min up to 30 min in a 2-min increment have been considered in stage 1 of a four-stage biosorption system for the sorption of N-NH_4^+. In the first biosorber, for example, system number 10 indicates that the first biosorber contact time is 2 min + (10-1)2 min = 20 min as system number 1 represents 2-min contact time in biosorber number 1. Hence, the contact time in the second biosorber, t_2, is the time, T min, required to achieve a fixed total percentage of N-NH_4^+ removal minus the contact time in the first biosorber stage t_1, therefore:

$$T = t_1 + t_2 \tag{24}$$

For N systems, t_n becomes

$$t_1 = 2 + (N - 1)2 \tag{25}$$

The total batch contact time, T, is

$$T = 2 + (N - 1)2 + t_2 \ldots t_n \tag{26}$$

where n is the number of stages.

The total contact time for each system number is calculated based on the fixed t_1 values for a particular percentage removal of N-NH_4^+.

Let us assume that the percentage removal in stage 2 is 50 %, stage 3 is 30 %, and stage 4 is 19 % in a 99 % removal of 40 mg/L N-NH_4^+ from 500 L aqueous solutions in a four-stage biosorption process (Fig. 6). The minimum contact time for the various system numbers for each batch biosorption stage was calculated using Eqs. (10)–(14) (Table 3). Each of the 15 systems representing the *x*-axes in Fig. 6 was based on a 2-min contact time interval in the first biosorber starting with system 1 at 2 min. A series of contact times from 2 min up to 30 min in a 2-min increment have been considered in stage 1 of a four-stage sorption system for the biosorption of N-NH_4^+. The optimum contact time (as shown in system number 4) for the biosorption of 99 % removal of 40 mg/L N-NH_4^+ from 500 L solution by *C. indica*/JOC is 75.89/95.16 min: with stage 1, 10/10 min; stage 2, 28.21/35.38 min; stage 3, 22.26/29.44 min; and stage 4, 17.42/22.34 min. Other varieties of percentage removal for the different stages were further used for optimization, for example, 50, 40 and 9 %; 60, 20 and 19 %; 60, 30 and 9 %; and 70, 20 and 9 % N-NH_4^+ removal for stages 1, 2, 3 and 4, respectively. The optimum contact time calculated from these varieties was not statistically different from the initial percentage variation for the different stages (Table 3). The process design demonstrated that a total contact time of 76 min or 96 min for *C. indica* or JOC, respectively, is required in each stage in a four-stage biosorption system for the sorption of 99 % N-NH_4^+ from 500 L solution containing 40 mg/L of the N-NH_4^+.

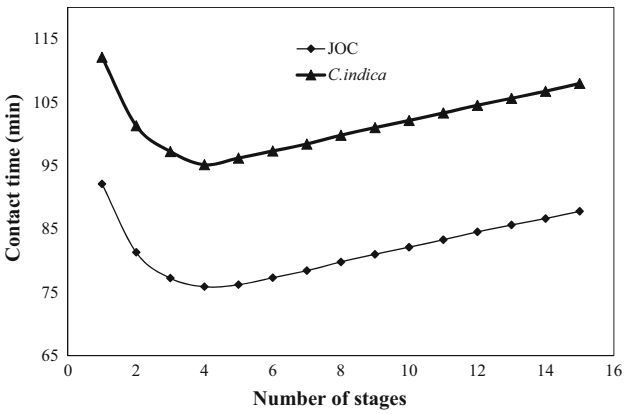

Fig. 6 Plots of optimized contact time and system number for the biosorption of 99 % of 40 mg/L N-NH_4^+ onto *C. indica* and JOC

Fourier transform infrared spectra analysis

The nature of the biosorbent–N-NH_4^+ interaction was elucidated on the basis of FT-IR. The FT-IR spectra of unloaded and NH_4–N-loaded form of both *C. indica* and JOC in the range of 400–4,000 cm^{-1} were taken (provided as supplementary data). The FT-IR spectrum of raw *C. indica* showed several distinct and sharp absorptions in the range of 33,431–3,808 cm^{-1} (indicative of hydroxyl groups), 2,925 cm^{-1} (indicative of -CH stretching), 2,367 cm^{-1} (indicative of C≡N nitrile bond), 1,630 cm^{-1} (indicative of C = O stretching), 1,525 cm^{-1} (indicative of imidazole ring), 1,431 cm^{-1} (indicative of carboxylate groups), 1,256 and 1,025 cm^{-1} (indicative of C–N-stretching) and the band at 1,161 cm^{-1} (indicative of –C–O stretching of ether groups) (Williams and Fleming 1991; Field et al. 2005). Similarly, the IR spectrum of raw JOC indicated absorption bands for hydroxyl groups (3,424 cm^{-1}), alkane or aliphatic C–H stretching (2,926 and 2,856 cm^{-1}), carbonyl groups (1,715 and 1,655 cm^{-1}), protein amide I and II (1,546 cm^{-1}), methoxy groups (1,459 and 1,419 cm^{-1}) and sulfur compounds (1,378, 1,059 and 1,159 cm^{-1}). The FT-IR spectra of *C. indica* exposed to NH_4-N indicated no shifts or change in any of the characteristic absorbance bands with the exception of a peak shift at 1,422, 1,250 and 1,157 cm^{-1} indicating carboxylate, C–O stretching in COOH group and O–H alcohols (primary and secondary), respectively. In addition, there was a new broad band between 3,650 and 3,900 cm^{-1} in the spectrum represents complexation of NH_4–N ions with the ionized O–H group of "free" hydroxyl groups and bonded O–H bands of carboxylic acids in the inter- and intramolecular hydrogen bonding of polymeric compounds (Wahab et al. 2010). These new bands and shifts indicated

Table 3 Optimized minimum contact time data (min) for the biosorption of 40 mg/L N-NH_4^+ from 500 L aqueous solution onto *C. indica*/JOC in a four-stage batch system

Percentage removal mode for stages 1, 2, 3 and 4, respectively	System no. Stage 4	Stage 1		Stage 2		Stage 3		Stage 4		Total	
		C. indica	JOC	*C. indica*	JOC	*C. indica*	JOC	*C. indica*	JOC	*C. indica*	JOC
50 %, 30 %, 19 %	4	8	8	28.21	35.38	22.26	29.44	17.42	22.34	75.89	95.16
50 %, 40 %, 9 %	4	8	8	28.21	35.38	20.64	27.94	19.93	24.58	76.78	95.90
60 %, 20 %, 19 %	4	8	8	25.86	33.45	24.73	31.67	17.56	22.39	76.15	95.51
60 %, 30 %, 9 %	4	8	8	25.84	33.41	22.29	29.39	19.91	24.52	76.04	95.32
70 %, 20 %, 9 %	3	6	6	27.57	34.61	24.73	31.63	19.97	24.49	78.27	96.73

that both carboxylic and hydroxyl groups played a major role in the removal of NH_4-N. The wave numbers of JOC after biosorption shifted from 2,373, 1,546 and 1,159 cm^{-1} to 2,370, 1,543 and 1,157 cm^{-1}, respectively, after ammonium biosorption. These peaks represented O–H stretch from strongly hydrogen-bonded –COOH, secondary –CONH and symmetric and asymmetric vibrations of $–SO_3^-$ groups, respectively (Benaissa and Elouchdi 2011). A new peak that was observed at 3,675 cm^{-1} was attributed to hydroxyl group, and it confirmed that N-NH_4^+ had been biosorbed by JOC. Although slight changes in the other absorption frequencies were observed, it was difficult to infer how these absorption peaks were related to N-NH_4^+ biosorption. The present results implied mainly involvement carboxylic and hydroxyl groups in biosorption of N-NH_4^+ ions by *C. indica*/JOC.

Scanning electron microscopy (SEM) micrographs of raw *C. indica* and JOC were obtained before and after ammonium biosorption onto *C. indica* and JOC (provided as supplementary data). The micrograph of N-NH_4^+-loaded biosorbents clearly showed the formation of cage-like structure in case of *C. indica* and presence of new shiny bulky particles adhering on the surface of JOC. These changes were absent before ammonium biosorption.

Conclusion

In the present study a seaweed biomass and a by-product from biodiesel recovery process were used for the removal of N-NH_4^+ from aqueous solution. The influence of suspension pH, contact time, biosorbent dose and initial concentration on N-NH_4^+ removal was investigated by conducting a series of batch biosorption experiments. The models based on the order of chemical reactions (pseudo-second-order and general rate law) accurately describe experimental points, which confirm the chemisorptive nature of the process. Also, Weber–Morris diffusive model correlates well with results indicating diffusion in the pores of the sorbent. External film transfer coefficients were in the order of 10^{-3} cm/s and internal diffusion coefficients were in the order of 10^{-8} cm^2/s for both the biosorbents. Based on the values of the Biot number, N-NH_4^+ biosorption onto both *C. indica* and JOC was controlled by internal pore resistance. A four-stage batch biosorber was designed based on the pseudo-second-order kinetics and was optimized to minimize the total contact time. The Fourier transform infrared spectroscopy (FTIR) analysis before and after biosorption of ammonium onto *C. indica* and JOC revealed involvement of carboxylic and hydroxyl functional groups.

Acknowledgments The authors wish to express their sincere thanks to Professor Bhavanath Jha, Discipline coordinator of Marine Biotechnology and Ecology for his valuable suggestions, Mr. Vinod Agrawal for FT-IR spectra and Mr. Jayesh Chaudhary for SEM analysis.

References

Aliabadi M, Khazaei I, Fakhraee H, Mousavian MTH (2012) Hexavalent chromium removal from aqueous solutions by using low-cost biological wastes: equilibrium and kinetic studies. Int J Environ Sci Technol 9:319–326

APHA (American Public Health Association) (1998) AWWA (American Water Works Association), WEF (Water Environment Federation), Standard methods for the examination of water and wastewater, 20th edn. APHA, Washington DC

Basha S, Murthy ZVP, Jha B (2009) Removal of Cu(II) and Ni(II) from industrial effluents by brown seaweed, *Cystoseira indica*. Ind Eng Chem Res 48:961–975

Benaissa H, Elouchdi MA (2011) Biosorption of copper (II) ions from synthetic aqueous solutions by drying bed activated sludge. J Hazard Mater 194:69–78

Boopathy R, Karthikeyan S, Mandal AB, Sekaran G (2013) Adsorption of ammonium ion by coconut shell-activated carbon from aqueous solution: kinetic, isotherm, and thermodynamic studies. Environ Sci Pollut Res 20:533–542

Buss SR, Herbert AW, Morgan P, Thornton SF, Smith WN (2004) A review of ammonium attenuation in soil and groundwater. Q J Eng Geol Hydrogeol 37:347–359

Chandra IK, Ju YH, Ayucitra A, Ismadji S (2012) Evans blue removal from wastewater by rarasaponin-bentonite. Int J Environ Sci Technol doi:10.1007/s13762-012-0114-y

Demir A, Gunay E, Debik E (2002) Ammonium removal from aqueous solution by ion exchange using packed bed natural zeolite. Water SA 28:329–336

Dizge N, Aydiner C, Demirbas E, Kobya M, Kara S (2008) Adsorption of reactive dyes from aqueous solutions by fly ash: kinetic and equilibrium studies. J Hazard Mater 150:737–746

Donmez D, Aksu Z (2002) Removal of chromium(VI) from saline wastewaters by *Dunaliella* species. Process Biochem 38:751–762

Emmerson KR, Russo RC, Luna RE, Thurston RV (1981) Aqueous ammonia equilibrium calculation: effect of pH and temperature. Can J Fish Aquat Sci 32:2379–2383

Fernando WARN, Xia K, Rice CW (2005) Sorption and desorption of ammonium from liquid swine waste in soils. Soil Sci Soc Am J 69:1057–1065

Field LD, Sternhell S, Kalman JR (2005) Organic structures from spectra, 3rd edn. Wiley, London, pp 64–68

Gupta S, Kumar D, Gaur JP (2009) Kinetic and isotherm modeling of lead(II) sorption onto some waste plant materials. Chem Eng J 148:226–233

Ho YS, McKay G (1998) A two-stage batch sorption optimized design for dye removal to minimize contact time. Trans IChemE 76B:313–318

Ho YS, McKay G (1999) Pseudo-second order model for sorption processes. Process Biochem 34:451–465

Jellali S, Wahab MA, Anane M, Riahi K, Jedidi N (2011) Biosorption characteristics of ammonium from aqueous solutions onto *Posidonia oceanica* (L.) fibers. Desalination 270:40–49

Ji ZY, Yuan JS, Li XG (2007) Removal of ammonium from wastewater using calcium form clinoptilolite. J Hazard Mater 141:483–488

Karadag D, Koc Y, Turan M, Armagan B (2006) Removal of ammonium ion from aqueous solution using Turkish clinoptilolite. J Hazard Mater B136:604–609

Komarowski S, Yu Q (1997) Ammonium ion removal from wastewater using Australian natural zeolite: batch equilibrium and kinetic studies. Environ Technol 18:1085–1097

Kumar D, Gaur JP (2011) Chemical reaction- and particle diffusion-based kinetic modeling of metal biosorption by a *Phormidium* sp.-dominated cyanobacterial mat. Bioresour Technol 102:633–640

Lagergren S (1898) About the theory of so-called adsorption of soluble substances. K Sven Vetenskapsakad Handl 24:1–39

Langmuir I (1918) The adsorption of gases on plane surfaces of glass, mica, and platinum. J Am Chem Soc 40:1361–1368

Lebedynets M, Sprynskyy M, Sakhnyuk I, Zbytniewski R, Golembiewski R, Buszewski B (2004) Adsorption of ammonium ions onto a natural zeolite: transcarpathian clinoptilolite. Adsorpt Sci Technol 22:731–741

Li Q, Yue QY, Sun HJ, Su Y, Gao BY (2010) A comparative study on the properties, mechanisms and process designs for the adsorption of non-ionic or anionic dyes onto cationic-polymer/bentonite. J Environ Manag 91:1601–1611

Lim S, Chu W, Phang S (2010) Use of *Chlorella vulgaris* for bioremediation of textile wastewater. Bioresour Technol 101:7314–7322

Liu Y, Liu YJ (2008) Biosorption isotherms, kinetics and thermodynamics. Sep Purif Technol 61:229–242

Liu Y, Wang Z-W (2008) Uncertainty of preset-order kinetic equations in description of biosorption data. Bioresour Technol 99:3309–3312

Liu H, Dong Y, Wang H, Liu Y (2010) Adsorption behavior of ammonium by a bioadsorbent-Boston ivy leaf powder. J Environ Sci 22:1513–1518

Namasivayam C, Sangeetha D, Gunasekaran R (2007) Removal of anions, heavy metals, organics and dyes from water by adsorption onto a new activated carbon from jatropha husk, an agro-industrial solid waste. Process Safe Environ Protect 85:181–184

Nethaji S, Sivasamy A, Mandal AB (2012) Adsorption isotherms, kinetics and mechanism for the adsorption of cationic and anionic dyes onto carbonaceous particles prepared from *Juglans regia* shell biomass. Int J Environ Sci Technol doi: 10.1007/s13762-012-0112-0

Okoniewska E, Lach J, Kacprzak M, Neczaj E (2007) The removal of manganese, iron and ammonium on impregnated activated carbon. Desalination 206:251–258

Ponnusami V, Rajan KS, Srivastava SN (2010) Application of film-pore diffusion model for methylene blue adsorption onto plant leaf powders. Chem Eng J 63:236–242

Rozic M, Cerjan-Stefanovic S, Kurajica S, Vancina V, Hodzic E (2000) Ammoniacal nitrogen removal from water by treatment with clays and zeolites. Water Res 34:3675–3681

Sun D, Zhang X, Wu Y, Liu T (2012) Kinetic mechanism of competitive adsorption of disperse dye and anionic dye on fly ash. Int J Environ Sci Technol. doi:10.1007/s13762-012-0130-y

Sutton MA, Oenema O, Erisman JW, Leip A, van Grinsven H, Winiwarter W (2011) Too much of a good thing. Nature 472:159–161

Thornton A, Pearce P, Parsons SA (2007) Ammonium removal from solution using ion exchange on to MesoLite, an equilibrium study. J Hazard Mater 147:883–889

Tosun I (2012) Ammonium removal from aqueous solutions by Clinoptilolite: determination of isotherm and thermodynamic parameters and comparison of kinetics by the double exponential model and conventional kinetic models. Int J Environ Res Public Health 9:970–984

Tuzun I, Bayramoglu G, Yalcm E, Basaran G, Celik G, Arıca MY (2005) Equilibrium and kinetic studies on biosorption of Hg(II), Cd(II) and Pb(II) ions onto microalgae *Chlamydomonas reinhardtii*. J Environ Manag 77:85–92

Urano K, Tachikawa H (1991) Process development for removal and recovery of phosphorus from wastewater by a new adsorbent. Ind Eng Chem Res 30:1897–1899

Vijayaraghavan K, Mao J, Yun YS (2008) Biosorption of methylene blue from aqueous solution using free and polysulfone-immobilized *Corynebacterium glutamicum*: batch and column studies. Bioresour Technol 99:2864–2871

Wahab MA, Jellali S, Jedidi N (2010) Ammonium biosorption onto sawdust: FTIR analysis, kinetics and adsorption isotherms modelling. Bioresour Technol 101:5070–5075

Weber WJ, Morris JC (1963) Kinetics of adsorption on carbon solution. J Sanit Eng Div ASCE 89:31–60

Williams DH, Fleming I (1991) Spectroscopic methods in organic chemistry. Tata McGraw-Hill Book Company Ltd., New Delhi, pp 40–76

Witek-Krowiak A (2011) Analysis of influence of process conditions on kinetics of malachite green biosorption onto beech sawdust. Chem Eng J 171:976–985

Wu D, Zhang B, Li C, Zhang Z, Kong H (2006) Simultaneous removal of ammonium and phosphate by zeolite synthesized from fly ash as influenced by salt treatment. J Colloid Interf Sci 304:300–306

Zheng Y, Wang A (2010) Preparation and ammonium adsorption properties of Biotite-based hydrogel composites. Ind Eng Chem Res 49:6034–6041

Zheng Y, Liu Y, Wang A (2011) Fast removal of ammonium ion using a hydrogel optimized with response surface methodology. Chem Eng J 171:1201–1208